Centrality dependence of high p_T hadron suppression in Au+Au collisions at $\sqrt{s_{\rm NN}}$=130 GeV

C. Adler[11], Z. Ahammed[23], C. Allgower[12], J. Amonett[14], B.D. Anderson[14], M. Anderson[5], G.S. Averichev[9], J. Balewski[12], O. Barannikova[9,23], L.S. Barnby[14], J. Baudot[13], S. Bekele[20], V.V. Belaga[9], R. Bellwied[31], J. Berger[11], H. Bichsel[30], A. Billmeier[31], L.C. Bland[2], C.O. Blyth[3], B.E. Bonner[24], A. Boucham[26], A. Brandin[18], A. Bravar[2], R.V. Cadman[1], H. Caines[33], M. Calderón de la Barca Sánchez[2], A. Cardenas[23], J. Carroll[15], J. Castillo[26], M. Castro[31], D. Cebra[5], P. Chaloupka[20], S. Chattopadhyay[31], Y. Chen[6], S.P. Chernenko[9], M. Cherney[8], A. Chikanian[33], B. Choi[28], W. Christie[2], J.P. Coffin[13], T.M. Cormier[31], J.G. Cramer[30], H.J. Crawford[4], W.S. Deng[2], A.A. Derevschikov[22], L. Didenko[2], T. Dietel[11], J.E. Draper[5], V.B. Dunin[9], J.C. Dunlop[33], V. Eckardt[16], L.G. Efimov[9], V. Emelianov[18], J. Engelage[4], G. Eppley[24], B. Erazmus[26], P. Fachini[2], V. Faine[2], J. Faivre[13], K. Filimonov[15], E. Finch[33], Y. Fisyak[2], D. Flierl[11], K.J. Foley[2], J. Fu[15,32], C.A. Gagliardi[27], N. Gagunashvili[9], J. Gans[33], L. Gaudichet[26], M. Germain[13], F. Geurts[24], V. Ghazikhanian[6], O. Grachov[31], V. Grigoriev[18], M. Guedon[13], E. Gushin[18], T.J. Hallman[2], D. Hardtke[15], J.W. Harris[33], T.W. Henry[27], S. Heppelmann[21], T. Herston[23], B. Hippolyte[13], A. Hirsch[23], E. Hjort[15], G.W. Hoffmann[28], M. Horsley[33], H.Z. Huang[6], T.J. Humanic[20], G. Igo[6], A. Ishihara[28], Yu.I. Ivanshin[10], P. Jacobs[15], W.W. Jacobs[12], M. Janik[29], I. Johnson[15], P.G. Jones[3], E.G. Judd[4], M. Kaneta[15], M. Kaplan[7], D. Keane[14], J. Kiryluk[6], A. Kisiel[29], J. Klay[15], S.R. Klein[15], A. Klyachko[12], A.S. Konstantinov[22], M. Kopytine[14], L. Kotchenda[18], A.D. Kovalenko[9], M. Kramer[19], P. Kravtsov[18], K. Krueger[1], C. Kuhn[13], A.I. Kulikov[9], G.J. Kunde[33], C.L. Kunz[7], R.Kh. Kutuev[10], A.A. Kuznetsov[9], L. Lakehal-Ayat[26], M.A.C. Lamont[3], J.M. Landgraf[2], S. Lange[11], C.P. Lansdell[28], B. Lasiuk[33], F. Laue[2], J. Lauret[2], A. Lebedev[2], R. Lednický[9], V.M. Leontiev[22], M.J. LeVine[2], Q. Li[31], S.J. Lindenbaum[19], M.A. Lisa[20], F. Liu[32], L. Liu[32], Z. Liu[32], Q.J. Liu[30], T. Ljubicic[2], W.J. Llope[24], G. LoCurto[16], H. Long[6], R.S. Longacre[2], M. Lopez-Noriega[20], W.A. Love[2], T. Ludlam[2], D. Lynn[2], J. Ma[6], R. Majka[33], S. Margetis[14], C. Markert[33], L. Martin[26], J. Marx[15], H.S. Matis[15], Yu.A. Matulenko[22], T.S. McShane[8], F. Meissner[15], Yu. Melnick[22], A. Meschanin[22], M. Messer[2], M.L. Miller[33], Z. Milosevich[7], N.G. Minaev[22], J. Mitchell[24], V.A. Moiseenko[10], C.F. Moore[28], V. Morozov[15], M.M. de Moura[31], M.G. Munhoz[25], J.M. Nelson[3], P. Nevski[2], V.A. Nikitin[10], L.V. Nogach[22], B. Norman[14], S.B. Nurushev[22], G. Odyniec[15], A. Ogawa[21], V. Okorokov[18], M. Oldenburg[16], D. Olson[15], G. Paic[20], S.U. Pandey[31], Y. Panebratsev[9], S.Y. Panitkin[2], A.I. Pavlinov[31], T. Pawlak[29], V. Perevoztchikov[2], W. Peryt[29], V.A Petrov[10], M. Planinic[12], J. Pluta[29], N. Porile[23], J. Porter[2], A.M. Poskanzer[15], E. Potrebenikova[9], D. Prindle[30], C. Pruneau[31], J. Putschke[16], G. Rai[15], G. Rakness[12], O. Ravel[26], R.L. Ray[28], S.V. Razin[9,12], D. Reichhold[8], J.G. Reid[30], G. Renault[26], F. Retiere[15], A. Ridiger[18], H.G. Ritter[15], J.B. Roberts[24], O.V. Rogachevski[9], J.L. Romero[5], A. Rose[31], C. Roy[26], V. Rykov[31], I. Sakrejda[15], S. Salur[33], J. Sandweiss[33], A.C. Saulys[2], I. Savin[10], J. Schambach[28], R.P. Scharenberg[23], N. Schmitz[16], L.S. Schroeder[15], A. Schüttauf[16], K. Schweda[15], J. Seger[8], D. Seliverstov[18], P. Seyboth[16], E. Shahaliev[9], K.E. Shestermanov[22], S.S. Shimanskii[9], V.S. Shvetcov[10], G. Skoro[9], N. Smirnov[33], R. Snellings[15], P. Sorensen[6], J. Sowinski[12], H.M. Spinka[1], B. Srivastava[23], E.J. Stephenson[12], R. Stock[11], A. Stolpovsky[31], M. Strikhanov[18], B. Stringfellow[23], C. Struck[11], A.A.P. Suaide[31], E. Sugarbaker[20], C. Suire[2], M. Šumbera[20], B. Surrow[2], T.J.M. Symons[15], A. Szanto de Toledo[25], P. Szarwas[29], A. Tai[6], J. Takahashi[25], A.H. Tang[14], J.H. Thomas[15], M. Thompson[3], V. Tikhomirov[18], M. Tokarev[9], M.B. Tonjes[17], T.A. Trainor[30], S. Trentalange[6], R.E. Tribble[27], V. Trofimov[18], O. Tsai[6], T. Ullrich[2], D.G. Underwood[1], G. Van Buren[2], A.M. VanderMolen[17], I.M. Vasilevski[10], A.N. Vasiliev[22], S.E. Vigdor[12], S.A. Voloshin[31], F. Wang[23], H. Ward[28], J.W. Watson[14], R. Wells[20], G.D. Westfall[17], C. Whitten Jr. [6], H. Wieman[15], R. Willson[20], S.W. Wissink[12], R. Witt[32], J. Wood[6], N. Xu[15], Z. Xu[2], A.E. Yakutin[22], E. Yamamoto[15], J. Yang[6], P. Yepes[24], V.I. Yurevich[9], Y.V. Zanevski[9], I. Zborovský[9], H. Zhang[33], W.M. Zhang[14], R. Zoulkarneev[10], A.N. Zubarev[9]

(STAR Collaboration)

[1]*Argonne National Laboratory, Argonne, Illinois 60439*
[2]*Brookhaven National Laboratory, Upton, New York 11973*
[3]*University of Birmingham, Birmingham, United Kingdom*
[4]*University of California, Berkeley, California 94720*
[5]*University of California, Davis, California 95616*
[6]*University of California, Los Angeles, California 90095*
[7]*Carnegie Mellon University, Pittsburgh, Pennsylvania 15213*
[8]*Creighton University, Omaha, Nebraska 68178*
[9]*Laboratory for High Energy (JINR), Dubna, Russia*
[10]*Particle Physics Laboratory (JINR), Dubna, Russia*
[11]*University of Frankfurt, Frankfurt, Germany*
[12]*Indiana University, Bloomington, Indiana 47408*
[13]*Institut de Recherches Subatomiques, Strasbourg, France*
[14]*Kent State University, Kent, Ohio 44242*

[15]*Lawrence Berkeley National Laboratory, Berkeley, California*
[16]*Max-Planck-Institut für Physik, Munich, Germany*
[17]*Michigan State University, East Lansing, Michigan 48824*
[18]*Moscow Engineering Physics Institute, Moscow Russia*
[19]*City College of New York, New York City, New York 10031*
[20]*Ohio State University, Columbus, Ohio 43210*
[21]*Pennsylvania State University, University Park, Pennsylvania*
[22]*Institute of High Energy Physics, Protvino, Russia*
[23]*Purdue University, West Lafayette, Indiana 47907*
[24]*Rice University, Houston, Texas 77251*
[25]*Universidade de Sao Paulo, Sao Paulo, Brazil*
[26]*SUBATECH, Nantes, France*
[27]*Texas A & M, College Station, Texas 77843*
[28]*University of Texas, Austin, Texas 78712*
[29]*Warsaw University of Technology, Warsaw, Poland*
[30]*University of Washington, Seattle, Washington 98195*
[31]*Wayne State University, Detroit, Michigan 48201*
[32]*Institute of Particle Physics, Wuhan, Hubei 430079 China and*
[33]*Yale University, New Haven, Connecticut 06520*
(Dated: June 18, 2002)

Inclusive transverse momentum distributions of charged hadrons within $0.2<p_T<6.0$ GeV/c have been measured over a broad range of centrality for Au+Au collisions at $\sqrt{s_{\rm NN}}$=130 GeV. Hadron yields are suppressed at high p_T in central collisions relative to peripheral collisions and to a nucleon-nucleon reference scaled for collision geometry. Peripheral collisions are not suppressed relative to the nucleon-nucleon reference. The suppression varies continuously at intermediate centralities. The results indicate significant nuclear medium effects on high p_T hadron production in heavy ion collisions at high energy.

PACS numbers: 25.75.-q

QCD predicts a phase transition at high energy density from hadronic matter to a deconfined Quark-Gluon Plasma (QGP) [1]. This transition may be studied in the laboratory through the collision of heavy ions at ultrarelativistic energies. Partons propagating in a medium lose energy through gluon bremsstrahlung [2–4], with the magnitude of the energy loss predicted to depend strongly on the gluon density of the medium. Measurement of partonic energy loss therefore provides a unique probe of the density of the medium.

Analysis of deep inelastic scattering and Drell-Yan pair production using nuclear targets indicates that the energy loss in cold nuclear matter is $0.2-0.5$ GeV/fm for quarks with energy greater than 10 GeV [5, 6]. Hard scattering of partons in nuclear collisions occurs early in the evolution of the extended system, thereby probing the phase of highest density. Energy loss softens the fragmentation of jets, leading to the suppression of high transverse momentum (high p_T) hadrons in the final state [7]. The PHENIX collaboration has reported the suppression of charged hadron and π^0 production at high p_T in central Au+Au collisions at center-of-mass energy per nucleon pair $\sqrt{s_{\rm NN}}$=130 GeV, relative both to reference data from nucleon-nucleon (NN) collisions and to peripheral Au+Au collisions [8]. The suppression is in qualitative agreement with predictions of partonic energy loss in dense matter, though quantitative conclusions require the understanding of other nuclear effects [8].

This Letter presents a measurement of the inclusive charged hadron yield $(\mathrm{h}^+ + \mathrm{h}^-)/2$ within $0.2<p_T<6.0$ GeV/c, measured for a broad range of centrality in Au+Au collisions at $\sqrt{s_{\rm NN}}$=130 GeV by the STAR collaboration at RHIC. Suppression of charged hadron production at high p_T in central collisions is observed, in qualitative agreement with the PHENIX measurement [8]. The high precision and wide kinematic and centrality coverage of the data presented here permit a detailed study of nuclear medium effects on hadron production from the soft to the hard scattering regime.

For comparison of spectra from nuclear collisions to an NN reference, the nuclear modification factor is defined as

$$R_{AA}(p_T) = \frac{d^2N^{AA}/dp_T d\eta}{T_{AA}\cdot d^2\sigma^{NN}/dp_T d\eta}, \qquad (1)$$

where T_{AA}=$\langle \mathrm{N_{bin}}\rangle/\sigma_{inel}^{NN}$ accounts for the collision geometry, averaged over the event centrality class. $\langle \mathrm{N_{bin}}\rangle$, the equivalent number of binary NN collisions, is calculated using a Glauber model. $R_{AA}(p_T)$ is less than unity at low p_T [9]. In contrast, the yield for hard processes scales as $\langle \mathrm{N_{bin}}\rangle$ in the absence of nuclear medium effects ($R_{AA}(p_T)$=1), and effects of the medium may be measured at high p_T by the deviation of $R_{AA}(p_T)$ from unity. In addition to final state energy loss, $R_{AA}(p_T)$ may be affected by initial state multiple scattering [7, 10] and transverse flow, both of which will enhance hadron production at high p_T, and by shadowing of nuclear parton distributions. At significantly lower $\sqrt{s}$ than the present study, enhancement of hadron production at high p_T has been observed in p-nucleus [11] and $\alpha-\alpha$ [12] collisions, as well as central collisions of heavy nuclei [13]. Current estimates of shadowing effects at RHIC energies contain large uncertainties [7, 14].

The STAR detector is described in [15]. Data collection utilized both a minimum bias trigger and a trigger selecting the 10% most central events. Charged particle tracks were detected in the Time Projection Chamber (TPC), with momentum determined from their curvature in a 0.25 T magnetic field. After event selection cuts, the central data set contained 320,000 events, while the minimum bias data set contained 240,000 events. The measured minimum bias distribution, corrected for vertex finding efficiency at low multiplicity, corresponds to $94\pm2\%$ of the Au+Au geometric cross section σ_{geom}^{AuAu}, assumed to be 7.2 barns [16].

Centrality selection is based on the primary charged particle multiplicity N_{ch} within the pseudorapidity range $|\eta|<0.5$. The most central bin is 0-5% of σ_{geom}^{AuAu}, while the most peripheral bin is 60-80%. Alternative centrality measures incorporate forward neutral energy [9, 17] and its correlation with multiplicity at midrapidity. The maximum variation of the p_T spectrum for different centrality measures is 4% for central events and less than 4% for more peripheral events. This variation is included in the systematic uncertainties of the reported spectra.

The hadron yield decreases rapidly with increasing p_T and its measurement is sensitive to small spatial distortions, which generate charge sign-dependent systematic errors in the measured track curvature. Measurement of the summed hadron yield, $(\mathrm{h}^+ + \mathrm{h}^-)/2$, is markedly less sensitive to such distortions than the yield of one charge sign alone. Each half of the cylindrical TPC is divided azimuthally into 12 sectors. High p_T tracks have small sagitta ($s \sim 0.8$ cm at p_T=5 GeV/c) and are confined to a single sector. For assessing systematic errors due to variation in detector response, each sector is considered to be an independent detector. The sector-wise distribution of $(\mathrm{h}^+ + \mathrm{h}^-)/2$ has a p_T-dependent rms variation of less than 5%, which is included in the systematic errors.

Analysis of inclusive charged particle spectra for p_T<2 GeV/c has been described previously [9]. Accepted tracks for p_T>2 GeV/c have $|\eta|<0.5$ and a distance of closest approach to the primary vertex less than 1 cm to reject background. Acceptance, efficiency, and momentum resolution were determined by embedding simulated tracks into real raw data events. For p_T>1.5 GeV/c, the Gaussian distribution of track curvature $k \propto 1/p_T$ has relative width $\delta k/k = 0.016 \cdot (p_T/(\mathrm{GeV}/c)) + 0.012$ for central events and $\delta k/k = 0.011 \cdot (p_T/(\mathrm{GeV}/c)) + 0.013$ for peripheral events. Correction was made for distortion due to finite momentum resolution. Typical correction factors are given in Table I.

Background corrections of significance are due to weak particle decays and anti-nucleon annihilation in detector material. The former are based on Λ, $\bar{\Lambda}$ and K_s^0 yields measured for $p_T < 2.5$ GeV/c [18, 19], with extrapolation to higher p_T using an exponential fit [18]. The latter are based on measured anti-proton yields [20]. The size of the net background correction is indicated in Table I. Systematic uncertainties in the final distributions were determined by varying the most sensitive cuts in the tracking and correction algorithms, and by varying the magnitude of the background contribution by 50% at $p_T \sim 2$ GeV/c and 100% at $p_T \sim 5.5$ GeV/c.

TABLE I: Typical multiplicative correction factors applied to the yields for peripheral and central collisions.

	p_T=2 GeV/c		p_T=5.5 GeV/c	
centrality	60-80%	0-5%	60-80%	0-5%
(Eff·Accept)$^{-1}$	1/0.86	1/0.63	1/0.88	1/0.67
Background	0.95	0.90	0.95	0.88
p_T-res. distortion	1.00	0.99	0.92	0.76

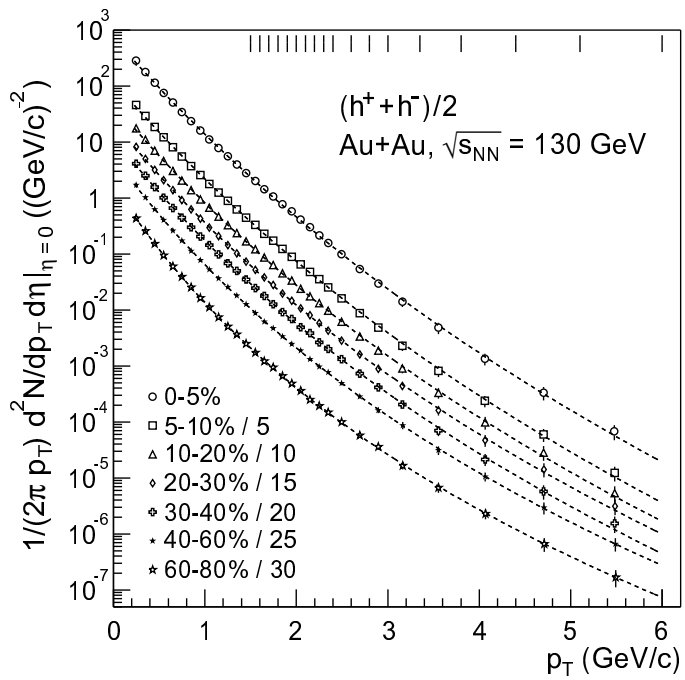

FIG. 1: Inclusive p_T distributions of $(\mathrm{h}^+ + \mathrm{h}^-)/2$. Non-central bins are scaled down by the indicated factors. The combined statistical and systematic errors are shown. Curves are fits to Eq. (2). Hash marks at the top indicate bin boundaries for p_T>1.5 GeV/c.

Figure 1 shows the inclusive p_T distributions of $(\mathrm{h}^+ + \mathrm{h}^-)/2$ within $|\eta|<0.5$ for various centrality bins, for Au+Au collisions at $\sqrt{s_{\mathrm{NN}}}$=130 GeV. Error bars, which are dominated by systematic uncertainties at all p_T, are generally smaller than the symbols. The spectra were fit by the pQCD-inspired power law function [21]

$$\frac{1}{2\pi p_T}\frac{dN}{dp_T} = C \cdot (1 + p_T/p_0)^{-n}, \qquad (2)$$

which describes p_T spectra of charged hadrons for NN collisions over a wide range of $\sqrt{s}$ [21–23]. Systematic changes in shape of the spectra with centrality are revealed by the fit parameters C, n, and mean transverse momentum $<p_T>=2p_0/(n-3)$ in Table II. Also shown in the Table are fit parameters for $\bar{\mathrm{p}} + \mathrm{p}$ collisions at $\sqrt{s}$=200 GeV [21]. Eq. (2) yields a poor fit relative to the errors for the most central bin, with systematic deviations from the fit function of 10-

TABLE II: Geometric quantities, charged particle density per participant pair, and fit parameters to Eq. (2), for various centrality bins and for $\bar{\mathrm{p}}+\mathrm{p}$ at 200 GeV [21], assuming σ_{inel}^{NN}=41 mb. The fits to the Au+Au data use uncorrelated measurement errors, which are largely systematic and non-Gaussian. Parameter errors shown also include correlated systematic uncertainties, which are added to parameter errors resulting from the fit.

centrality	$\langle \mathrm{N_{bin}} \rangle$	$\langle \mathrm{N_{part}} \rangle$	$\frac{dN_{ch}}{d\eta}$	$\frac{2}{\langle \mathrm{N_{part}} \rangle}\frac{dN_{ch}}{d\eta}$	Power Law Fit ($0.2 < p_T < 6.0$ GeV/c)		
					$C((\mathrm{GeV}/c)^{-2})$	$< p_T >$ (GeV/c)	n
0-5%	965^{+67}_{-67}	350^{+4}_{-4}	563±39	3.22±0.23	797±60	0.520±0.010	21.9±0.5
5-10%	764^{+59}_{-63}	296^{+7}_{-7}	452±32	3.05±0.23	654±50	0.517±0.010	20.7±0.4
10-20%	551^{+48}_{-56}	232^{+9}_{-9}	344±24	2.96±0.24	520±40	0.511±0.010	18.9±0.4
20-30%	348^{+44}_{-45}	165^{+10}_{-10}	234±16	2.83±0.26	372±28	0.504±0.011	17.3±0.3
30-40%	210^{+36}_{-36}	115^{+10}_{-12}	144±10	2.51±0.30	252±19	0.497±0.011	17.2±0.3
40-60%	90^{+22}_{-22}	62^{+9}_{-11}	72.2±5.1	2.35±0.42	141±11	0.480±0.011	14.8±0.2
60-80%	20^{+7}_{-9}	20^{+5}_{-6}	21.0±1.5	2.13±0.61	50±4	0.446±0.011	13.0±0.2
$\bar{\mathrm{p}}+\mathrm{p}$(200)	1	2	2.65 ± 0.08	2.65 ± 0.08	7.7±0.4	0.392±0.003	11.8±0.4

20%, whereas for more peripheral collisions it fits well, with parameters tending smoothly to those for $\bar{\mathrm{p}}+\mathrm{p}$ collisions.

A more direct comparison of yields for different centralities relies on estimating $\langle \mathrm{N_{bin}} \rangle$ and the mean number of participants $\langle \mathrm{N_{part}} \rangle$ for each centrality bin. For this purpose, the distribution $d\sigma/d\mathrm{N_{bin}}$ (and equivalently, $d\sigma/d\mathrm{N_{part}}$) was calculated using a Monte Carlo Glauber model [17] with σ_{inel}^{NN}=41 $\pm$ 1 mb and Woods-Saxon nuclear matter density, using radius $r = 6.5 \pm 0.1$ fm and surface diffuseness $a = 0.535 \pm 0.027$ fm. [16]. Percentile intervals of $d\sigma/d\mathrm{N_{bin}}$ (calculated) and $d\sigma/dN_{ch}$ (measured) were equated to extract $\langle \mathrm{N_{bin}} \rangle$ for each centrality bin. The Glauber model parameters and geometric cross section were varied to estimate the systematic uncertainties. Results are given in Table II.

Because charged particle distributions at midrapidity are used for centrality selection, biases in the relation between $d\sigma/d\mathrm{N_{bin}}$ and $d\sigma/dN_{ch}$ due to fluctuations and autocorrelations were assessed. Variation of parameters in a Monte Carlo calculation of multiplicity fluctuations for fixed collision geometry, and comparison of the measured multiplicity distribution in an azimuthal quadrant centered on a high p_T particle against those in the other quadrants, both yielded negligible uncertainties in $\langle \mathrm{N_{bin}} \rangle$ and $\langle \mathrm{N_{part}} \rangle$.

Table II shows the charged particle yield per participant pair, $\frac{2}{\langle \mathrm{N_{part}} \rangle}\frac{dN_{ch}}{d\eta}$, obtained by integrating the p_T spectra. The extrapolated yield in p_T<0.2 GeV/c is $\sim$ 20% of the total for all centralities. The dependence of $\frac{2}{\langle \mathrm{N_{part}} \rangle}\frac{dN_{ch}}{d\eta}$ on $\langle \mathrm{N_{part}} \rangle$ is consistent with observations in [17].

Figure 2 shows the ratio of the central (0-5%) spectrum to that of the two peripheral bins (40-60%, 60-80%), normalized by $\langle \mathrm{N_{bin}} \rangle$. The dashed lines at unity and below show scaling with $\langle \mathrm{N_{bin}} \rangle$ and $\langle \mathrm{N_{part}} \rangle$ respectively, and the shaded regions show the systematic uncertainties from Table II. The vertical error bars on the data points are the uncertainties of the central data, while the horizontal caps are the quadrature sum of the uncertainties of both data sets. Approximate participant scaling at low p_T is seen. The ratio rises monotonically below $p_T \sim 2$ GeV/c and decreases at high p_T. The ratio of central over most peripheral achieves a value at p_T=5.5 GeV/c of 0.27±0.12 with additional uncertainty ±0.12 due to $\langle \mathrm{N_{bin}} \rangle$, establishing significant suppression of charged hadron production at high p_T in central collisions.

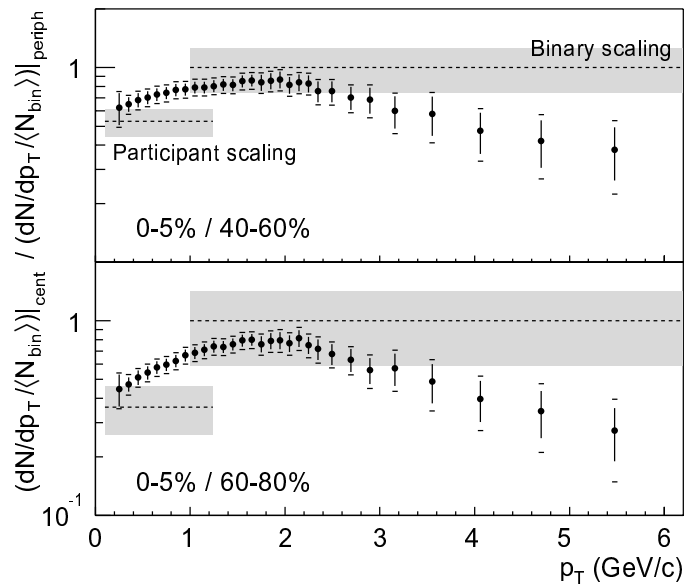

FIG. 2: Ratio of charged hadron yields within $|\eta| < 0.5$ for central over peripheral collisions, normalized to $\langle \mathrm{N_{bin}} \rangle$.

Figure 3 shows $R_{AA}(p_T)$ for various centrality bins relative to an NN reference spectrum, parameterized by Eq. (2) with $C\sigma_{inel}^{NN} = 267^{+4}_{-6}$ mb/(GeV/c)^2, $p_0 = 1.90^{+0.17}_{-0.09}$ GeV/c, and $n = 12.98^{+0.92}_{-0.47}$ (the superscripts and subscripts are curves that bound the systematic uncertainty). The reference was determined by fitting Eq. (2) to UA1 $\bar{\mathrm{p}}+\mathrm{p}$ data at $\sqrt{s}$=200-900 GeV [21] and extrapolating to $\sqrt{s}$=130 GeV. Extrapolation of the 200 GeV spectrum to 130 GeV using pQCD calculations agrees to within 5% with the reference at p_T=6 GeV/c [25, 26]. Correction to the NN reference for the UA1 acceptance ($|\eta|$<2.5), which differs from this analysis ($|\eta|$<0.5),

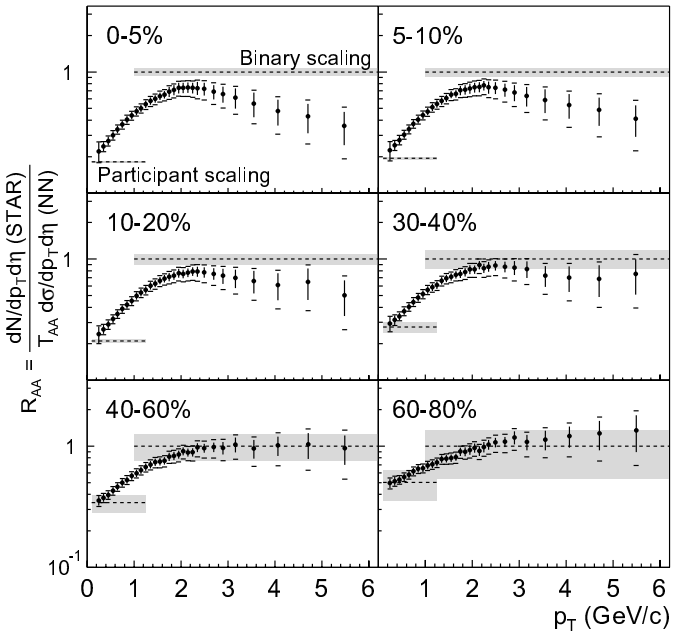

FIG. 3: $R_{AA}(p_T)$ for various centrality bins, for Au+Au relative to an NN reference spectrum. Error bars are described in the text. Errors between different p_T and centrality bins are highly correlated.

was based on two independent pQCD calculations [25, 27], giving a multiplicative correction of 1.17 ± 0.06 at p_T=2.0 GeV$/c$ and 1.35 ± 0.10 at p_T=5.5 GeV$/c$. The p_T-dependent systematic uncertainty of the NN reference is the quadrature sum of the power law parameter and the acceptance correction uncertainties. Isospin effects are negligible for p_T<6 GeV$/c$ [26]. The error bars are the systematic uncertainties of the measured spectra, while the caps show their quadrature sum with the systematic uncertainty of the NN reference.

$R_{AA}(p_T)$ increases monotonically for p_T<2 GeV$/c$ at all centralities, and saturates near unity for p_T>2 GeV$/c$ in the most peripheral bins. In contrast, $R_{AA}(p_T)$ for the central bins reaches a maximum and then decreases strongly above p_T=2 GeV$/c$, showing suppression of the charged hadron yield relative to the NN reference of 0.36 ± 0.17 (sys) at p_T=5.5 GeV$/c$ for the 0-5% bin, with additional uncertainty ± 0.03 due to $\langle \mathrm{N_{bin}} \rangle$. $R_{AA}(p_T)$ varies continuously as a function of centrality, and no centrality threshold for the onset of suppression is observed [28].

In summary, charged hadron production in high energy collisions of heavy nuclei has been studied over a wide range of p_T and event centrality. At high p_T, hadron yields scale with the number of binary collisions for peripheral collisions, while significant suppression of hadron production is seen for central collisions. STAR has also reported large azimuthal anisotropy at high p_T [29]. These phenomena indicate substantial energy loss of the final state partons or their hadronic fragments in the medium generated by high energy nuclear collisions, though quantitative measurement of this effect requires additional reference data.

We thank the RHIC Operations Group and the RHIC Computing Facility at Brookhaven National Laboratory, and the National Energy Research Scientific Computing Center at Lawrence Berkeley National Laboratory for their support. This work was supported by the Division of Nuclear Physics and the Division of High Energy Physics of the Office of Science of the U.S. Department of Energy, the United States National Science Foundation, the Bundesministerium für Bildung und Forschung of Germany, the Institut National de la Physique Nucléaire et de la Physique des Particules of France, the United Kingdom Engineering and Physical Sciences Research Council, Fundação de Amparo à Pesquisa do Estado de São Paulo, Brazil, the Russian Ministry of Science and Technology and the Ministry of Education of China and the National Science Foundation of China.

[1] J. W. Harris and B. Müller, Ann. Rev. Nucl. Part. Sci. **46**, 71 (1996).
[2] M. Gyulassy and M. Plümer, Phys. Lett. **B243**, 432 (1990).
[3] X. N. Wang and M. Gyulassy, Phys. Rev. **D44**, 3501 (1991); Phys. Rev. Lett. **68**, 1480 (1992).
[4] M. Gyulassy and X. N. Wang, Nucl. Phys. **B420**, 583 (1994); R. Baier, D. Schiff and B. G. Zakharov, Ann. Rev. Nucl. Part. Sci. **50**, 37 (2000).
[5] E. Wang and X. N. Wang, hep-ph/0202105.
[6] F. Arleo, Phys. Lett. **B532**, 231 (2002).
[7] X. N. Wang, Phys. Rev. **C61**, 064910 (2000);
[8] K. Adcox *et al.*, Phys. Rev. Lett. **88**, 022301 (2002).
[9] C. Adler *et al.*, Phys. Rev. Lett. **87**, 112303 (2001).
[10] G. Papp *et al.*, Nucl. Phys. **A698**, 627c (2002).
[11] D. Antreasyan *et al.*, Phys. Rev. **D19**, 764 (1979).
[12] A. L. S. Angelis *et al.*, Phys. Lett. **B185**, 213 (1987).
[13] M. M. Aggarwal *et al.*, Eur. Phys. J. **C23**, 225 (2002).
[14] S. Li and X. N. Wang, Phys. Lett. **B527**, 85 (2002).
[15] C. Adler *et al.*, Nucl. Instr. Meth. **A**, RHIC Special Volume, in press.
[16] A. J. Baltz *et al.*, Nucl. Instr. Meth. **A417**, 1 (1998).
[17] B. B. Back *et al.*, Phys. Rev. **C65**, 031901(R) (2002); K. Adcox *et al.*, Phys. Rev. Lett. **86**, 3500 (2001); I. G. Bearden *et al.*, Phys. Lett. **B 523**, 227 (2001);
[18] C. Adler *et al.*, nucl-ex/0203016.
[19] C. Adler *et al.*, nucl-ex/0206008.
[20] C. Adler *et al.*, Phys. Rev. Lett. **87**, 262302 (2001); K. Adcox *et al.*, Phys. Rev. Lett. **88**, 242301 (2002).
[21] C. Albajar *et al.*, Nucl. Phys. **B335**, 261 (1990).
[22] B. Alper *et al.*, Nucl. Phys. **B100**, 237 (1975).
[23] F. Abe *et al.*, Phys. Rev. Lett. **61**, 1819 (1988).
[24] D. Kharzeev and M. Nardi, Phys. Lett. **B507**, 121 (2001).
[25] T. Sjöstrand *et al.*, Comp. Phys. Comm. **135**, 238 (2001).
[26] I. Vitev, private communication.
[27] F. Yuan, private communication; A. Polleri and F. Yuan, nucl-th/0108056.
[28] X. N. Wang, Phys. Rev. **C63**, 054902 (2001).
[29] C. Adler *et al.*, nucl-ex/0206006.